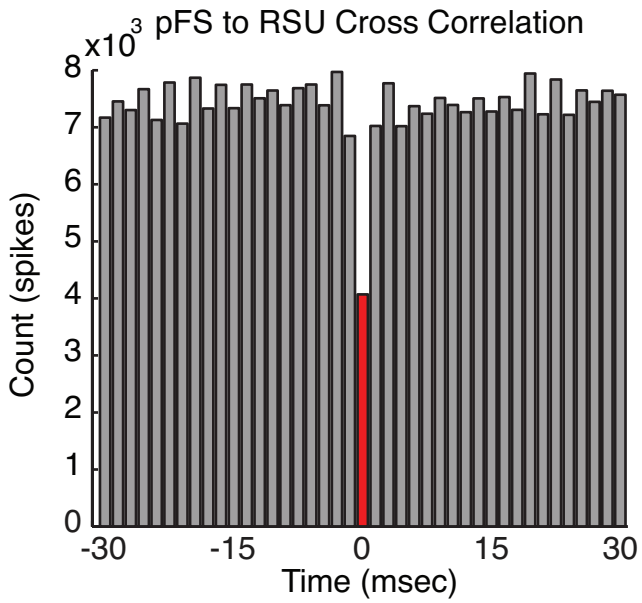

Figure S1 (Associated with Figure 1)

Supplemental Figure S1 (assoc. w/ Fig. 1) Example pFS/RSU spike cross correlation. Spike times from pairs of pFS interneurons and RSUs recorded on the same wire were cross correlated to confirm that the activity of pFS interneurons was consistent with an inhibitory cell type. For each pFS spike, all RSU spikes 30 msec before and after the pFS spike were summed in 1.5 msec bins. Each bar represents the number of RSU spikes that occurred in that time bin (1.5 msec/bar) relative to a the pFS spike at time 0. The pFS/RSU cross correlation indicates a decrease in the number of RSU spikes occurring between 0 and 1.5 msec immediately after a pFS spike fired (red bar).

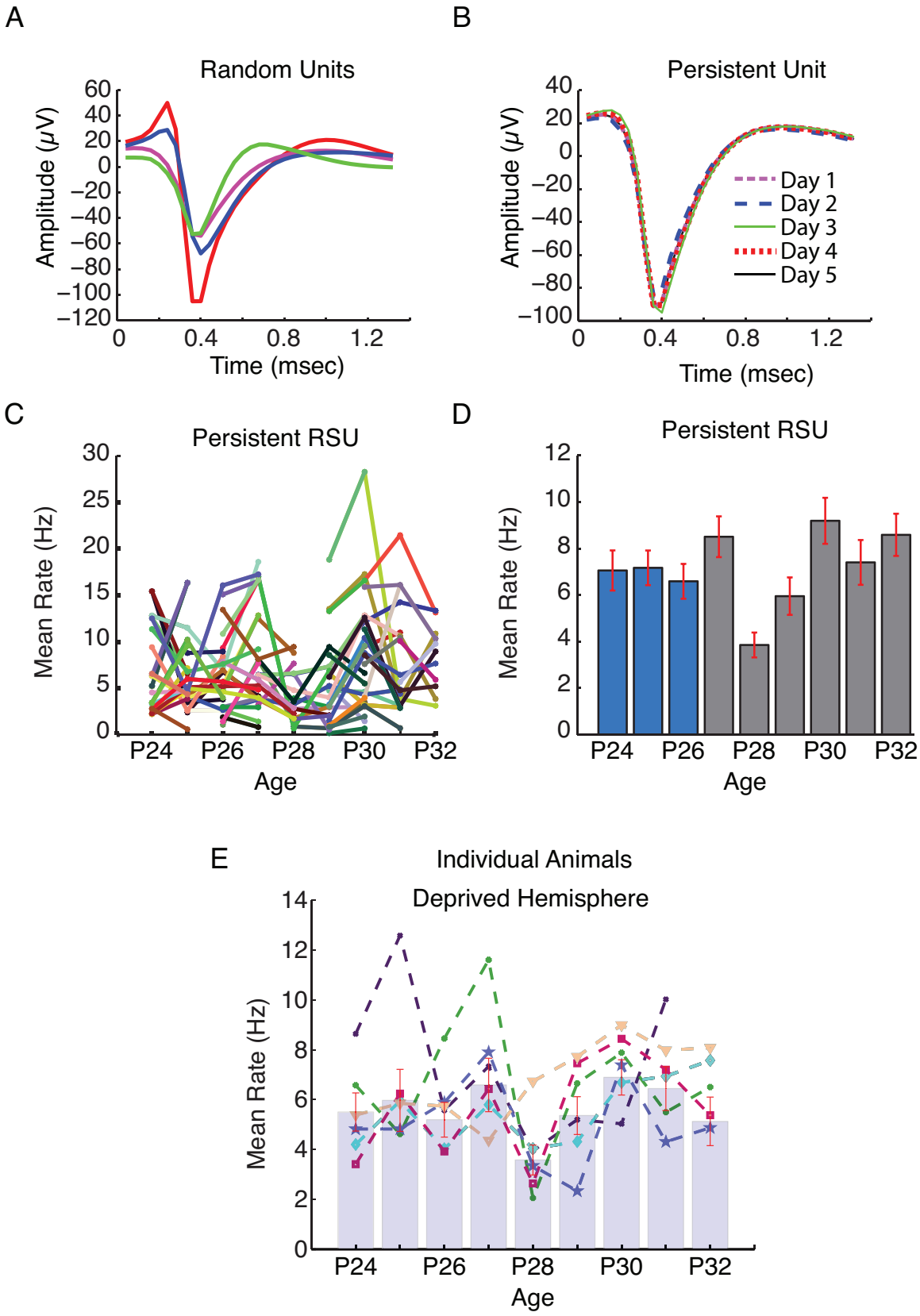

Figure S2 (Associated with Figure 2)

Supplemental Figure S2 (assoc. w/ Fig. 2) Persistent units and individual animal effects. A subset of cells were reliably identifiable across multiple days of recording. (A) The mean waveform of randomly selected single units demonstrates a high degree of variability in individual unit waveforms. (B) An algorithm compared mean waveforms as well as the rate and probability of waveform drift in order to select single units across days. Illustrated is the mean waveform of an identified persistent unit across 5 days of recording. (C) Overlay of individual persistent unit means. To isolate a more stable population of neurons, we included only those cells that were persistent across at least 2d of recording (see supplemental methods). (D) The persistent RSU response to MD was nearly identical to the entire dataset; firing rates dropped on MD2 and returned to baseline levels by MD6 (ANOVA, $p<0.05$). (E) This biphasic response to MD was observed at the level of the individual animals studied here (dashed colored lines represent single animals, grey bars represent the mean across animals). One animal for which we did not have units for all 8 days was omitted from this analysis. All error bars indicate ±SEM.

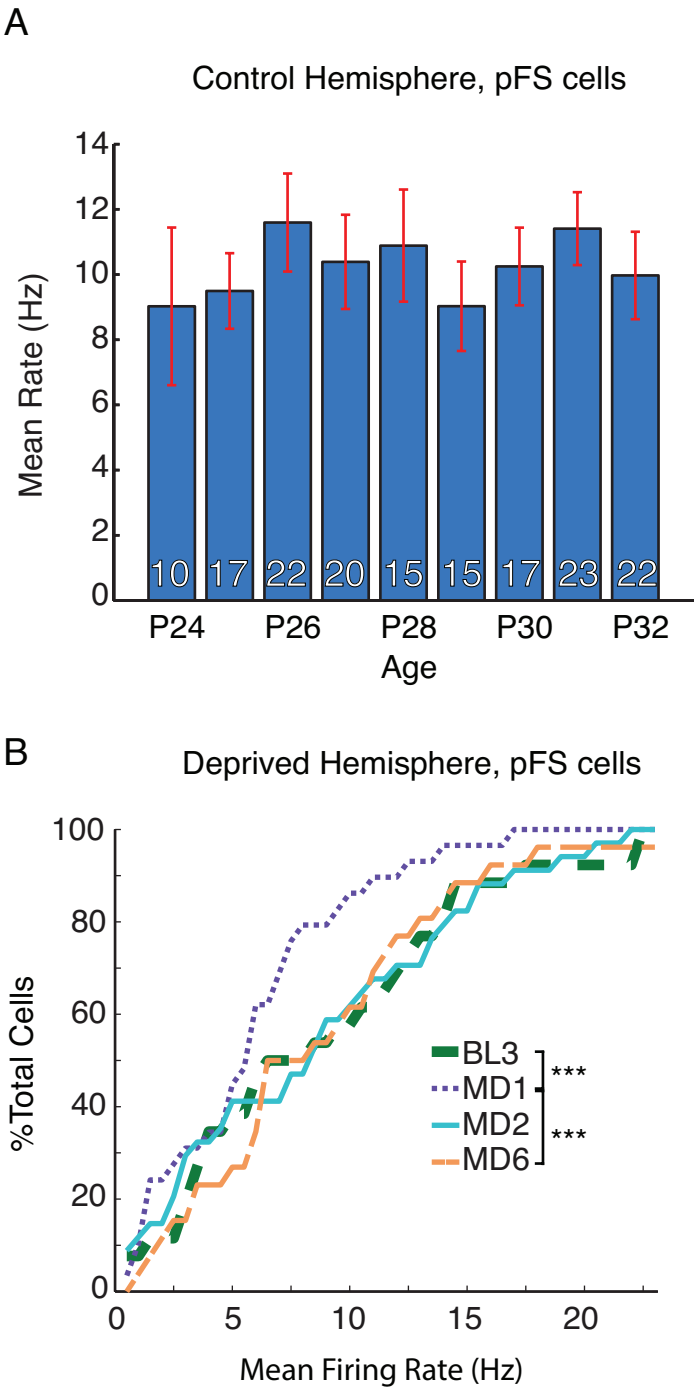

Figure S3 (Associated with Figure 3)

Supplemental Figure S3 (assoc. w/ Fig. 3) pFS control and cumulative firing rates during deprivation. (A) pFS cells measured in the non-deprived hemisphere showed no significant changes in mean firing rate across 9 days of recording (ANOVA, $p=0.91$). White numbers in bars indicate the number of cells. (B) A cumulative probability plot of mean pFS interneuron firing rates demonstrates a significant shift towards lower rates on MD1 compared to baseline (KS test, $p<0.001$). This effect reversed by MD2. The firing rate distribution was then stable through MD6. All error bars indicate ±SEM.

Supplemental Detailed Experimental Procedures

All protocols followed the National Institutes of Health Guide for the Care and Use of Laboratory Animals and were in compliance with institutional guidelines.

Surgery and multiunit recording

Long Evans rats of both sexes (n=7, Charles River, 21 days old at the time of surgery) were used in these experiments. Rats were implanted bilaterally in monocular primary visual cortex (V1m, centered approximately 3.5 mm lateral and 1.5 mm caudal from lambda) under ketamine/xylazine anesthesia (100 and 10 mg/kg, respectively). Electrode arrays were custom manufactured 16-channel polyimide tungsten microwire arrays cut to 5 different lengths spanning a 1mm range in order to record from multiple cortical layers simultaneously (Tucker-Davis Technologies, Alachua, FL, wire diameter 33 μm, electrode spacing 250 μm, row

separation 375 μm, tip angle 45°). Arrays were implanted using a stereotax in accordance with Katz *et al.* (2001) and Piette *et al.* (2012). One day prior to surgery, experimental animals and two littermates were acclimated to the recording chamber for 4 hours.

The surgical procedure was performed in a sterile surgery suite using autoclaved and Cetylcide sterilized materials. After preparing the dorsal surface of the skull, two 750 μm diameter holes were drilled, one above the cerebellum and the other above the fronto/parietal region (1mm caudal and 2 mm lateral to Bregma) to support 760 μm diameter stainless steel machine screws. A 1 x 2 mm craniotomy was drilled over V1m using 1.0 mm and 0.45 mm drill bits with the aid of a high-speed dental drill. Dura was excised with a 25-gauge needle and 45° #5 forceps (Fine Science Tools, Foster City, CA, part number 11251-35).

The electrode array was advanced until the shortest wires were penetrating the most superficial surface of cortical tissue. The final insertion depth was ~ 1.1 mm below the cortical surface for the longest set of wires (layer 5/6) and ~ 0.1 mm for the shortest wires (approximately superficial layer 2). The craniotomy and implanted array were then sealed with either petroleum jelly or silicone gel (Dow Corning, 3-4680). A small amount of dental acrylic was used to fix the array to the skull. While this hardened (~10 minutes), two 450 μm holes were drilled (1mm caudal to the craniotomy and 1 mm rostral to the craniotomy) for the insertion of differential ground and reference wires, each of which protruded into brain by 1 mm. Ground and reference holes were then filled with either petroleum jelly or silicone gel (Dow Corning), and then covered with dental acrylic. The dental acrylic

"head cap" was then built up with a hollow core using Pasteur pipettes. This arrangement minimized the total "head cap" weight (~1.35g including arrays and machine screws).

Following surgery, animals were housed individually for 48h in transparent plastic cages with a heating pad and *ad libitum* access to food and water. Recording began at noon on the third day following surgery (postnatal day 24). Animals were placed in the recording chamber with two littermates. The recording chamber (12"x12", plexiglass) was lined with 1.5" of bedding and provided *ad libitum* access to food and water. Additionally, animals were provided with unique environmental enrichment on each day of recording in order to promote exploration and activity. Lighting and temperature were kept constant (LD 12:12, lights on at 7:30 am, 20° C).

Signal processing and data analysis

Data were acquired with a Tucker-Davis Neurophysiology Workstation (Tucker-Davis). Continuous data (25 kHz) were streamed to disc for offline LFP and spike extraction using custom software (MATLAB). Spikes were initially extracted from high pass filtered raw data (500 Hz) based on an amplitude threshold (-5 standard deviations from the mean signal). When a sample crossed the threshold, the 8 preceding and 24 following sample points and time stamps (33 total) were extracted and saved for future principal components analyses and waveform clustering. Offline spike sorting was performed in custom software (MATLAB). The first four principal components were extracted to

create feature vectors and clustering was performed using the KlustaKwik algorithm for spike separation in high dimensional feature space (Harris *et al.*, 2000). This algorithm fits a mixture of Gaussians with covariance matrices and is based on the CEM algorithm (Celeux and Govaert, 1992). Identified units were scored on a 3-point quality scale based on the L-ratio and Mahalanobis distance (Schmitzer-Torbert *et al.*, 2005) of each cluster of waveform projections in 4-dimensional eigenspace. Additionally, single units were separated from multiunit traces by asymmetrical waveforms, the presence of an obvious refractory period (as assessed by the autocorrelation of spike times within a single cluster), and an after hyperpolarization (observed as an "overshoot" of baseline voltage following each spike). The stability of identified units was assessed by comparing the mean squared error of the mean waveform in the first ten minutes of recording to the mean waveform in the last ten minutes of recording. Any unit with a sum MSE of greater than 30 μV was discarded from these analyses as we could not be confident that the unit represented a single cell. The signal to noise ratio in our system was sufficiently high that we were regularly able to resolve multiple individual units on single wires. Due to the duration of the daily recordings, our data captured some units that we were not able to reliably detect throughout an entire recording session. Units whose activity was below our ability to discriminate from noise across the first or last hour of an 8h recording were excluded from analyses (<2% of units). Regular spiking units (RSUs) and putative fast-spiking interneurons (pFS cells) were discriminated based on the spiking kinetics (Niell and Stryker, 2008). A plot of peak to trough time versus the waveform slope 250 to 570 μsec after the minimum revealed a bimodal distribution. Based on this, pFS cells were defined as those single units with a peak to trough time of less than 450 μsec and

negative waveform slope (see above). pFS cells had higher average firing rates and shorter mean interspike intervals than RSUs.

To identify the subset of cells that could be reliably identifiable across multiple days, we developed an algorithm that selected units recorded on individual wires across multiple days and compared the sum MSE of waveforms between units. Units whose mean waveforms drifted beyond a conservative threshold across an 8h recording were rejected from the persistent pool. Only those pairs of units recorded on consecutive days with a sum inter-unit MSE below than the threshold for single unit drift/day were included.

For examination of ISI distributions we restricted our analyses to those between 0 and 1 second (~95% of the total distribution), to eliminate occasional artifacts due to momentary losses of recorded signal during very aggressive play.

Histological Reconstruction

After the 6th day of monocular deprivation, animals were heavily anesthetized with ketamine xylazine and current was passed through each wire of the implanted arrays (7V for 3 sec). The animal was then perfused intracardially with 4% paraformaldehyde and the brain was removed. Brains were stored in a 30% sucrose solution for >7d before being sliced at 60 μm on a freezing sliding microtome. Slices were stored overnight in PBS and then mounted to glass slides. Slides were allowed to dry overnight and then stained with cresyl violet to dye Nissl substance in the cytoplasm of neurons. Stained slices were photomicrographed and examined in order for the location and layer of each wire in the array. Units recorded on wires

outside of V1m were excluded from these analyses. To confirm the accuracy of histological layer estimation in one animal, we delivered pulses of full field green light (50x50msec at 1 Hz) after the animal was dark adapted each night. The LFP (low pass filtered at 300 Hz) was subjected to current source density analysis. As expected, wires in layer 4 (as assessed by depth and post-mortem reconstruction) demonstrated a significant current sink, wires in layer 2/3 showed a mixed response, and wires in layer 5 demonstrated a current source.

Behavioral Analyses

Video of animal behavior was collected through the duration of recordings and scored for behavioral state offline. Animal behavior was divided into three categories: 'Active Wake', which included any locomotor activity such as play and exploration, 'Quiet Wake', which included grooming, quiescent periods with small movements and obvious postural stability, and 'Sleep', which included long periods of motionless quiescence and lack of postural tone. The distributions of behavioral states between implanted animals and littermates were similar. Behavioral scoring was compared to the LFP delta band power (1 to 4 Hz, Chebyshev Type II filter, MATLAB) to confirm the accuracy of sleep scoring in a subset of animals (n=3). All behaviorally scored epochs of sleep demonstrated increases in delta band power.

In vitro slice recordings

Slices were cut in chilled (1° C) modified artificial cerebrospinal fluid (mACSF). mACSF was continuously oxygenated and contained (in mM): 110 choline

chloride, 25 $NaHCO_3$, 25 dextrose, 11.6 sodium ascorbate, 7 $MgCl_2$, 3.1 sodium pyruvate, 2.5 KCl, 1.25 NaH_2PO, and 0.5 $CaCl_2$; after cutting, slices were incubated in room temperature oxygenated standard ACSF containing (in mM): 126 NaCl, 3 KCl, 2 $MgSO_4$, 1.25 $NaHPO_4$, 25 $NaHCO_3$, 2 $CaCl_2$, 25 dextrose until use. V1m was identified and whole-cell patch clamp recordings obtained from L2/3 pyramidal neurons as described (Lambo and Turrigiano, 2013). Internal recording solution contained (in mM): 20 KCl, 100 K-gluconate, 10 HEPES, 4 Mg-ATP, 0.3 Na-GTP, 10 phosphocreatine, and 0.2% biocytin; neurons were voltage-clamped to -70 mV in standard ACSF containing TTX (0.2 μM), APV (50μM), and picrotoxin (25μM) and warmed to 33ºC. Neurons were excluded from analyses if Vm was > -60 mV, Rin was < 80 MΩ, Rs was > 20 MΩ, or if any of these parameters changed by more than 10% during the recording. Pyramidal neurons were identified by the presence of an apical dendrite and tear-drop shaped soma and morphology was confirmed by *post hoc* reconstruction of biocytin fills. All physiology data were analyzed using in-house programs written in IgorPro (Wavemetrics).

Supplemental Citations

Celeux G, Govaert G (1992). A classification algorithm for clustering and two stochastic versions. *Computational Statistics and Data Analysis*. 14, 315-332.
Desai NS, Cudmore RH, Nelson SB, Turrigiano GG (2002). Critical periods for experience-dependent synaptic scaling in visual cortex. *Nat Neurosci.* 5(8):783-9.
Harris KD, Henze Da, Csicsvari J, Hirase H, Buzsake G (2000). Accuracy of tetrode spike separation as determined by simultaneous intracellular and extracellular measurements. *J Neurophysiol.* 84(1):401-14.
Katz DB, Simon SA, Nicolelis MAL (2001). Electrophysiological studies of gustation in awake rats. In: Methods and Frontiers in the Chemical Senses (Simon SA, Nicolelis MAL, eds), pp 339-357. Boca Raton, FL: CRC.
Maffei A, Lambo ME, Turrigiano GG (2010). Critical period for inhibitory plasticity in rodent binocular V1. *J Neuosci.* 30(9):3304-9.

Nataraj K, Turrigiano G (2011). Regional and temporal specificity of intrinsic plasticity mechanisms in rodent primary visual cortex. *J Neurosci.* 31(49):17932-40.
Niell CM, Stryker MP (2008). Highly selective receptive fields in mouse visual cortex. *J Neurosci.* 28(30):7520-36.
Piette CE, Baez-Santiago MA, Reid EE, Katz DB, Moran A (2012). Inactivation of basolateral amygdala specifically eliminates palatability-related information in cortical sensory responses. *J Neurosci.* 32(29):9981-91.
Schmitzer-Torbert N, Jackson J, Henze D, Harris K, Redish AD (2005). Quantitative measures of cluster quality for use in extracellular recordings. *Neuroscience.* 131(1):1-11.